Self-organized criticality in single-neuron excitability

Asaf Gal[1,2,*] and Shimon Marom[2,3]

[1]*The Interdisciplinary Center for Neural Computation (ICNC), The Hebrew University, Jerusalem, Israel*

[2]*Network Biology Research Laboratories, Lorry Lokey Interdisciplinary Center for Life Sciences and Engineering, Technion, Haifa, Israel*

[3]*Department of Physiology, Faculty of Medicine, Technion, Haifa, Israel*

(Received 1 November 2012; revised manuscript received 7 August 2013; published 18 December 2013)

We present experimental and theoretical arguments, at the single-neuron level, suggesting that neuronal response fluctuations reflect a process that positions the neuron near a transition point that separates excitable and unexcitable phases. This view is supported by the dynamical properties of the system as observed in experiments on isolated cultured cortical neurons, as well as by a theoretical mapping between the constructs of self-organized criticality and membrane excitability biophysics.

DOI: 10.1103/PhysRevE.88.062717 PACS number(s): 87.18.−h, 87.19.L−

I. INTRODUCTION

Cellular excitability is a fundamental physiological process whereby voltage-dependent changes in exciting and restoring membrane ionic conductances lead to an *action potential* (AP), a transient change in transmembrane voltage. Hodgkin and Huxley [1] formalized a generic biophysical mechanism underlying the ignition and propagation of action potentials. In this formalism, as well as in its later extensions, the flow of ions down their electrochemical gradients is modulated by the probability of ion channel proteins to reside in a conductive state. An extensive set of observations shows that the activity and response properties of neurons are highly variable, fluctuating over extended time scales in a complex manner (see, e.g., Refs. [2–4]) that are not easily accounted for by either the original Hodgkin-Huxley formalism nor by its extensions, i.e., by adding more ionic currents, gates, and channel states (see Ref. [5]). Several approaches have been suggested for explaining these fluctuations, largely focusing on the stochastic nature of underlying mechanisms [6–9], nonlinearity and chaotic dynamics [10,11], or network level effects [12].

This paper approaches variability and complexity in single-neuron activity from a different viewpoint. Conventional analyses and models of excitability use dynamical system approaches [13]. However, excitability is known to be an emergent property of coupled states of numerous interacting microscopic elements—ion channels, calling for a statistical-mechanics description. While clues do exist for the potential benefit of thinking about excitability in statistical-mechanics terms (for instance, voltage fluctuations near the spiking bifurcation point, in biophysical models of excitability, were shown to exhibit critical-like behavior [14,15]), such an approach has not yet been explicitly proposed. Here we apply the framework of self-organized criticality (SOC) to the level of a single, individual neuron, treated as an ensemble of *interacting ion channels*.

Originally introduced into the study of neural systems as a framework for explaining distributions of durations and sizes of network-wide events of activity ("avalanches") in cultured neural networks [16], SOC has since been applied to *in vivo* recordings at the network and whole-brain levels [17]. Acknowledging the controversies that surround its experimental foundations [18,19], SOC provides an attractive theoretical framework for explaining the emergence of complexity in neural dynamics, establishing intriguing links to a long tradition of statistical-mechanics treatment of neural networks [20]. However, all of these studies treated the neural network as an ensemble of interacting *neurons*, markedly different from the study presented here, which considers the neuron as an isolated physical system. The relevance of our ideas to brain dynamics remains to be determined.

II. SUMMARY OF EXPERIMENTAL OBSERVATIONS

In a series of experiments, detailed in a previous publication [4], the intrinsic dynamics of excitability was observed by monitoring the responses of single neurons to a series of pulse stimulations. In brief, cortical neurons from newborn rats were cultured on multielectrode arrays, allowing extracellular recording and stimulation for long, practically unlimited durations. The neurons were isolated from their network by means of pharmacological synaptic blockage to allow study of intrinsic excitability dynamics, with minimal interference of coupled cells. Neurons were stimulated with sequences of short, suprathreshold identical electric pulses. For each pulse, the binary response (AP produced or not) was registered, marking the neuron as residing in either an *excitable state* or an *unexcitable* state. For each AP recorded, the *latency* from stimulation to the AP was also registered. The amplitude of the stimulating pulses was constant and set well above threshold, such that the neuron would respond in a 1:1 manner (i.e., every stimulation pulse produces an AP) under a low rate (1 Hz) stimulation condition.

When the stimulation rate r is increased to values higher than 1 Hz, two distinct response regimes can be identified: a *stable* regime, in which each stimulation elicits an AP, and an *intermittent* regime, in which the spiking is irregular. The response of a neuron following a change of stimulation rate is demonstrated in Figs. 1(a) and 1(b), as well as in Ref. [4]: When the stimulation rate is abruptly increased to a higher value, the latency gradually becomes longer and stabilizes on a new value. For high enough stimulation rate (above a critical value r_0), the 1:1 response mode breaks down and becomes intermittent. All transitions are fully reversible.

*Corresponding author: asaf.gal@mail.huji.ac.il

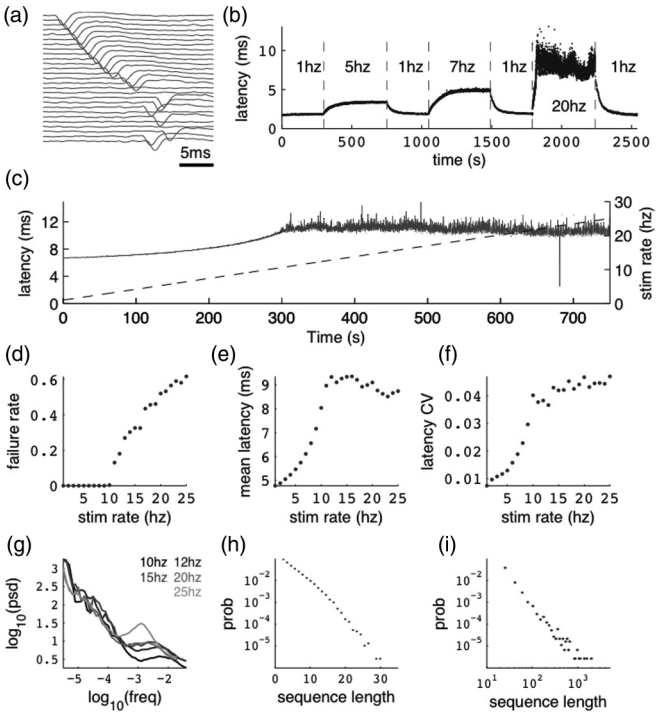

FIG. 1. Experimental observation of excitability dynamics. (a) The response of a single isolated neuron to sequences of pulse stimuli delivered at 20 Hz. The responses are ordered top to bottom; every 20th response is shown for clarity. The delaying of the AP can be observed, as well as response failures when excitability is below threshold. (b) The AP latency plotted as a function of time in an experiment where the stimulation rate is changed. For low stimulation rates, the excitability stabilizes at a fixed, suprathreshold value. For a high stimulation rate (20 Hz), the excitability decreases below threshold, and the neuron responds intermittently. (c) Response latencies (solid line) in response to a stimulation sequence with slowly increasing stimulation rate (dashed line). (d) Failure (no spike) probability as a function of stimulation rate. A critical stimulation rate is clearly evident. (e) Mean response latency as a function of stimulation rate. The increase of the latency accelerates as the stimulation rate approaches the critical point. (f) The jitter (coefficient of variation) of the latency as a function of stimulation rate. (g) Scale-free fluctuations in the intermittent mode. Periodograms of the failure rate fluctuations, at five different stimulation rates above r_0. (h) Length distribution of spike-response sequences on a semilogarithmic plot, demonstrating an exponential behavior. Example from one neuron stimulated at 20 Hz for 24 h. (i) Length distribution of no-spike response sequences from the same neuron, on a double logarithmic plot, demonstrating a power-law-like behavior.

The steady state properties of the two response regimes may be observed by slowly changing the stimulation rate. As seen in the result of the "adiabatic" experiment [Fig. 1(c)], the stable regime is characterized by a 1:1 response (no failures), stable latency (low jitter), and monotonous dependency of latency on the stimulation rate. In contrast, the intermittent regime is characterized by a failure rate that increases with the stimulation rate, unstable latency (high jitter), and independence of the mean latency on the stimulation rate. The existence of a critical (or threshold) stimulation rate is reflected in measures of the failure rate [Fig. 1(d)], the mean latency [Fig. 1(e)], and the latency coefficient of variation [Fig. 1(f)]. The exact value of r_0 varies considerably between neurons, but its existence is observed in practically all measured neurons (see details in Ref. [4]).

Within the intermittent regime, the fluctuations of excitability (as defined by the excitable/unexcitable state sequence) are characterized by scale-free long-memory statistics. Its power spectral density (PSD) exhibits a power-law ($1/f^{\beta}$) tail at the low frequency domain. The characteristic exponent of this power law does not depend on the stimulation rate, as long as the latter is kept above r_0 [Fig. 1(g)]. The typical exponent of the rate PSD is $\beta = 1.26 \pm 0.21$ (mean $\pm$ SD, calculated over 16 neurons). Moreover, within the intermittent regime, the distributions of the lengths of consecutive response sequences (i.e., periods of time the neuron is fully excitable, responding to each stimulation pulse) and consecutive no-response sequences (i.e., periods of time the neuron is not responding) are qualitatively different [Figs. 1(h) and 1(i)]. The consecutive response sequence length histogram is strictly exponential, having a characteristic duration, while the consecutive no-response sequence length histogram is wide, to the point of scale-freeness. Likelihood ratio tests for power-law distribution fit to the empirical histogram (containing 90 000 samples) yielded significantly more likelihood compared with exponential fit, log normal, stretched exponential, and linear combination of two exponential distributions (all with normalized log likelihood ratios of $R > 10$, $p < 0.001$, see Ref. [21]). This suggests that the fluctuations are dominated by widely distributed excursions into an unexcitable state.

III. INTERPRETATION

In what follows we suggest an interpretation to the origin of the above experimental results in terms of critical phenomena, accounting for the complex statistics of single neuron excitability over extended time scales. The concept of 'excitability' is vaguely defined; it generally reflects the susceptibility of the cell to produce an action potential in response to input above a given amplitude. In that sense, a "nonexcitable" cell is one that can not evoke an AP, regardless of the stimulation amplitude, while an "excitable" cell is characterized by a continuous measure that quantifies excitability. Such a measure can be, for example, the minimal stimulation amplitude required for evoking an AP (the threshold) or alternatively the latency of the evoked AP, a more easily observed measure which is tightly related to the threshold.

Excitability is a lumped product of the individual states of numerous interacting ion channels: the aggregated macroscopic availability of these ionic channels to move into the conductive state and participate in the generation of action potentials. In the short term, the total number of ionic channels that are available to participate in AP generation may safely be assumed to be a constant. In the original Hodgkin and Huxley formalism, aims at the scale of milliseconds, the latter assumption is translated to maximal conductance *parameters* that set limits on the instantaneous dynamics of the membrane. However, when long-term effects are sought, the maximal conductance might (and indeed should) be treated as a macroscopic system variable governed by stochastic, activity-dependent, transitions of ion channels into and out of

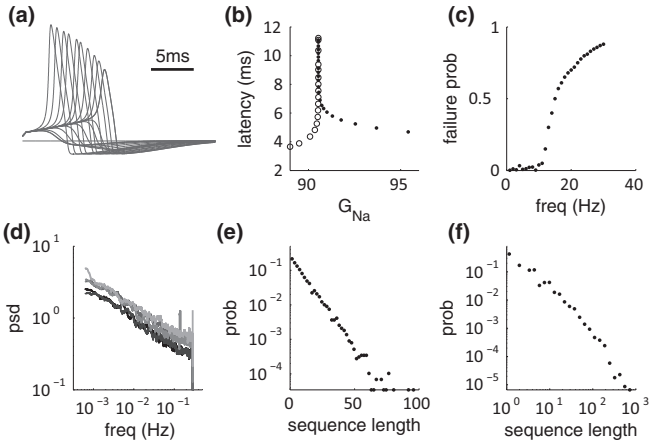

FIG. 2. (a) The effect of modulating G_{Na} in the Hodgkin-Huxley model under short pulse stimulation. As it decreases, the AP is delayed. Below a certain threshold, no AP is produced. (b) AP latency in panel (a) as a function of G_{Na}, demonstrating the existence of a sharp threshold. Propagating APs are marked with solid circles; nonpropagating responses are marked with empty circles. (c) Simulation results of the contact process model [Eq. (2)]. Dependence of the spike failure probability on the stimulation rate, analogous to Fig. 1(d). (d) Power spectral densities of the response fluctuations at different frequencies above the r_0, $1/f$-type behavior. (e) Length distribution of spike-response sequences, on a semilogarithmic plot, demonstrating an exponential behavior, analogous to Fig. 1(h). (f) Length distribution of no-spike response sequences from the same neuron, on a double logarithmic plot, demonstrating a power-law-like behavior, analogous to Fig. 1(i).

long-lasting *unavailable* states. These transitions are globally and locally coupled via membrane voltage, ionic concentrations, and cellular modulatory and homeostatic processes. Since unavailable channels cannot contribute to membrane electrical response, slow changes in maximal conductance will be reflected in the time-amplitude envelope of the generated action potential, as well as in the very ability to generate it. The precise impacts of slow changes in maximal conductances on excitability depend upon the specific type of ionic channel involved (i.e., mediating exciting or restoring ionic flows). Figures 2(a) and 2(b) exemplify this point for the case of sodium maximal conductance. Such observed excitability has the flavor of an order parameter, a measurable macroscopic physical quantity that reflects an average over the individual states of elements in an ensemble. The complex irregularity of neuronal responses over extended time scales, observed in the experiments described above, is thus naturally interpreted as a reflection of residency of the system near a phase transition between excitable and unexcitable phases, giving rise to the observed power-law statistics.

However, given the above interpretation of fluctuations in excitability as reflecting critical phenomena, one would expect to observe the critical characteristics within a limited range of the experimental control parameter (i.e., stimulation rate); higher values of stimulation rate should shut down excitability altogether. This is not the case. For example, Figs. 1(e) and 1(g) show that response latency and the characteristic exponent of the power spectral density are insensitive to the stimulation rate. The reason for this apparent inconsistency is that the stimulation rate does not directly impact the dynamics of the underlying ionic channels. Rather, the relevant control parameter is in fact the *activity* rate, itself a dynamic variable of the system. This suggests a form of *self-organization*.

The concept of SOC [22] designates a cluster of physical phenomena characterizing systems that reside near a phase transition. What makes SOC unique is the fact that residing near a phase transition is not the result of a fine-tuned control parameter; rather, in SOC the system positions itself near a phase transition as a natural consequence of the underlying internal dynamic process that pushes towards the critical value. Such systems exhibit many complex statistical and dynamical features that characterize behavior near a phase transition, without these features being sensitive to system parameters. Dickman and his colleagues [23,24] formalized a scheme for generating SOC from a conventional system exhibiting a phase transition. They have shown that many of the canonical models of SOC, including sandpile and forest fire models, can be understood as systems exhibiting absorbing-state phase transitions. Systems such as the contact process or activated random walk may reside about the phase transition, if amended with a carefully designed feedback: dissipating energy whenever the system is supercritical (i.e., permanently active without settling into an absorbing state) and driving the system whenever it is subcritical (i.e., when and only when it settles into the absorbing state).

This picture naturally maps into excitability dynamics, where neural activity serves as a temperaturelike parameter, and the single AP serves as a drive (quantal influx of energy or a small increase in temperature). In the absence of activity, the neuron reaches an excitable state (the "absorbing state" in such a mapping), while increased activity reduces excitability and (when high enough) pushes the membrane into the unexcitable state. Residency in the unexcitable state decreases neural activity, leading to the restoration of excitability. As a result, the neuron is kept around a barely excitable state, exhibiting characteristics of SOC. Of course, not all classes of neurons follow this simplistic process, but the general idea holds: activity pushes excitability towards a threshold state, while at the longer time scale regulatory feedback pulls the system back.

IV. MODEL

The above interpretation of excitability in SOC terms may also be theoretically supported, within certain limits, by considering the underlying biophysical machinery. The state of the membrane is a function of the individual states of a large population of interacting ion channel proteins. A single ion channel can undergo transformations between uniquely defined conformations, conventionally modeled as states in a Markov chain. The faster transition dynamics between states is the foundation of the Hodgkin-Huxley model, which describes the excitation event itself—the action potential. But, as explained above, for the purpose of modeling the dynamics of excitability, rather than the generative dynamics of the action potential itself, it is useful to group these conformations into two sets [9,11,25,26]: the *available*, in which channels can participate in the generation of action potentials, and the *unavailable*, in which channels are deeply inactivated and

are "out of the game" of action potential generation. The microscopic details of the single-channel dynamics in this state space, and definitely the collective dynamics of the interacting ensemble, are complex [27–29] and no satisfactory embracing model exists to date. However, it has been suggested recently [11,26] that the transition dynamics between the available and unavailable states may be expressed in terms of an "adaptive rate," logisticlike model of the general form

$$\dot{x} = -f(\gamma)x + g(x)(1-x), \tag{1}$$

where f is a function of the neural activity measure γ, and $g(x)$ is a monotonically increasing function of the system state x, which represents the gross availability of ion channels. In this modeling approach, complex transition statistics are a result of ensemble-level interaction, rather than of the internal structure of the single-channel state space.

Following the lead of the above adaptive rate approach, one can consider, for instance, a model in which x represents the availability of a restoring (e.g., potassium) conductance [30]. The state of the single channel is represented by a binary variable σ_i; $\sigma_i = 0$ is the unavailable state and $\sigma_i = 1$ is the available state. Unavailable channels are recruited with a rate of x, while available channels are lost with a rate of $2-\gamma$. This picture gives rise to a dynamical mean-field-like equation:

$$\dot{x} = (\gamma - 1)x - x^2. \tag{2}$$

The model is a variant of a globally coupled contact process, a well-studied system exhibiting an absorbing-state phase transition [31]. Here, $x = 0$ is the absorbing state, representing the excitable state of the system. In the artificial case of γ as an externally modified control parameter, for $\gamma < 1$ (low activity) the system will always settle into this state, and the neuron will sustain this level of activity. For $\gamma > 1$, the system will settle on $x^* = \gamma - 1$, an unexcitable state, and the neuron will not be able to sustain activity. Feedback is introduced into the system by specifying the state dependency of γ: An AP is fired if and only if the system is excitable (i.e., in the absence of restoring conductance, $x = 0$), giving rise to a small increase in γ. When $x > 0$, the system is unexcitable, APs are not fired, and γ is slowly decreased. This is an exact implementation of the scheme proposed in Refs. [23,24]: an absorbing-state system, where the control parameter (activity, γ) is modified by feedback from the order parameter (excitability, a function of x).

As always with SOC, the distinction between order and control parameters becomes clear only when the conservative, open-loop version of the model is considered. Note that the natural dependency of the driving event (the AP) on the system state in our neural context resolves a subtlety involved in SOC dynamics: the system must be driven slowly enough to allow the absorbing state to be reached, before a new quantum of energy is invested. In most models, this condition is met by taking the driving rate to be infinitesimally small.

Numerical simulation of the model [Eq. (2), together with the closed loop dynamics of γ, see the Appendix] qualitatively reproduces the power-law statistics observed in the experiment, including the existence of a critical stimulation rate r_0 [Fig. 2(c)], the $1/f$ behavior for $r > r_0$, with an exponent independent on r [Fig. 2(d)], and the distributions of sequence durations [Figs. 2(e) and 2(f)]. The model has three relevant parameters: the integration time scale τ_γ of neural activity, the quantum of activity ($d\gamma$) added following each AP, and the stimulation rate r. The critical stimulation rate r_0 is adjustable by changing the first two parameters, and the SOC behavior is observed for any $r > r_0$, under the condition that $\tau_\gamma \gg 1/r_0$. While the model does capture key observed properties, others are not accounted for. The latency transient dynamics when switching between stimulation rates [Fig. 1(b)] and the multitude of stable latency values for $r < r_0$ [Fig. 1(c)] suggest that a model with a single excitable state is not sufficient. Sandpile models (and more generally activated random walk models, see Refs. [23,24]), do exhibit such multiplicity, arising due to a continuum of stable subcritical values of pile height (or slope). In this analogy, adding grains to the pile increases its height up to the critical point, where SOC is observed. Another experimentally observed property that is not accounted for by the model is the existence of *pattern modes* in the intermittent response regime as described in Fig. 10 of Ref. [4], implying strong temporal correlations between events of excitability and unexcitability. These temporal correlations affect the exponent of the power-law spectral density and might explain the difference between the exponent in the experiment and in the model simulation. Such correlations are not alien to SOC and might arise in variant models [32].

V. CONCLUDING COMMENTS

We have given several arguments, experimental and theoretical, in support of a connection between the framework of SOC and the dynamics underlying response fluctuations in single neurons. This interpretation succeeds in explaining critical-like fluctuations of neuronal responsiveness over an extended time scale, which are not accounted for by other, more common, approaches [5,33]. The key component that enables SOC in the ion channel ensemble is the existence of interchannel interaction. While the interaction chosen here is *global*, there is evidence that *short range* cooperation (as is more abundant in physical models of SOC) also exists between ion channels [34] and might be used to construct alternative models. Naturally, the simple model leading to Eq. (2) is not unique, and is probably wrong in its microscopical details. Moreover, excitability is determined by more than one order parameter, and the interaction types are much more heterogeneous, controlled by an aggregate of such equations, representing the exciting and restoring forces, each pushing-pulling excitability to opposite directions.

Nevertheless, while respecting the gap between theoretical models and biological reality, SOC seems to capture the core phenomenology of fluctuating neuronal excitability and has the potential to enhance our understanding of the physiological aspects of excitability dynamics.

ACKNOWLEDGMENTS

The authors thank Erez Braun, Dani Dagan, and Yariv Kafri for insightful comments and discussions. The research leading to these results has received funding from the European Union's Seventh Framework Programme (FP7/2007-2013) under Grant agreement No. FP7-269459 CORONET, and was also supported by a grant from the Ministry of Science & Technology, Israel, and funding organization of EU countries.

APPENDIX: MATERIALS AND METHODS

1. Cultured neurons experiments

Experiments were performed on cultures of cortical neurons of newborn rats, as described in Refs. [4,35]. Neurons were cultured on multielectrode arrays, allowing for extracellular recording of neuronal activity and extracellular electrical stimulation. As described in Ref. [4], experiments were performed under complete blockage of synaptic transmission to allow the study of intrinsic excitability dynamics in isolation from the effect of the activity of other neurons. Neurons were stimulated with sequences of short (400 μs) pulse stimulations from one of the electrodes, with a fixed interstimulus interval. Following each pulse, the response of the neurons was recorded (from a different electrode): whether a spike was fired or not, and the latency of the response from the stimulation pulse. While the effect of the stimulation is local to the part of the neuron near the stimulation electrode, the latency to the response reflects the conductance properties along the neuron from the stimulation electrode to the recording one, usually hundreds of microns away. Careful measures were applied [4] to exclude experimental instabilities' modulation of the response of neurons over time.

2. Hodgkin-Huxley model simulation

A Hodgkin-Huxley model neuron [Figs. 2(a) and 2(b)] was simulated using standard dynamic and rate equations [36]. The neuron was stimulated with an injected rectangular current pulse (500 μs duration, 50 μA amplitude), and the voltage dynamics was observed. The leak conductance G_L was set to 0.3 mS, the potassium conductance G_K was set to 28 mS, and the sodium conductance G_{Na} was changed in the range of 80–110 mS.

3. Contact process simulation

The simulation was performed using an ensemble of 10 000 channels. The loop on neuronal activity γ was closed as follows: for each AP fired, a single channel was inactivated, and γ was increased by a value of $d\gamma = 0.005$. Between APs, γ decayed exponentially with a rate of 0.001. The simulation length was 1 h for each stimulation rate for Fig. 2(c), and 12 h for each stimulation rate for Figs. 2(d)–(F). The full MATLAB code of the simulation can be accessed at the authors' website [37].

[1] A. L. Hodgkin and A. F. Huxley, J. Physiol. **117**, 500 (1952).
[2] S. B. Lowen and M. C. Teich, J. Acoust. Soc. Am. **99**, 3585 (1996).
[3] M. C. Teich, C. Heneghan, S. B. Lowen, T. Ozaki, and E. Kaplan, J. Opt. Soc. Am. A **14**, 529 (1997).
[4] A. Gal, D. Eytan, A. Wallach, M. Sandler, J. Schiller, and S. Marom, J. Neurosci. **30**, 16332 (2010).
[5] D. Soudry and R. Meir, Front. Comput. Neurosci. **6**, 4 (2012).
[6] E. Schneidman, B. Freedman, and I. Segev, Neural Comput. **10**, 1679 (1998).
[7] S. B. Lowen, L. S. Liebovitch, and J. A. White, Phys. Rev. E **59**, 5970 (1999).
[8] Y. Soen and E. Braun, Phys. Rev. E **61**, R2216 (2000).
[9] G. Gilboa, R. Chen, and N. Brenner, J. Neurosci. **25**, 6479 (2005).
[10] H. Korn and P. Faure, C. R. Biol. **326**, 787 (2003).
[11] S. Marom, Front. Comput. Neurosci. **3**, 2 (2009).
[12] C. van Vreeswijk and H. Sompolinsky, Science **274**, 1724 (1996).
[13] E. M. Izhikevich, *Dynamical Systems in Neuroscience* (MIT Press, Cambridge, MA, 2007), p. 441.
[14] M. A. D. Roa, M. Copelli, O. Kinouchi, and N. Caticha, Phys. Rev. E **75**, 021911 (2007).
[15] D. A. Steyn-Ross, M. L. Steyn-Ross, M. T. Wilson, and J. W. Sleigh, Phys. Rev. E **74**, 051920 (2006).
[16] J. M. Beggs and D. Plenz, J. Neurosci. **23**, 11167 (2003).
[17] D. R. Chialvo, Nat. Phys. **6**, 744 (2010).
[18] N. Dehghani, N. G. Hatsopoulos, Z. D. Haga, R. A. Parker, B. Greger, E. Halgren, S. S. Cash, and A. Destexhe, Front. Physiol. **3**, 302 (2012).
[19] C. Bédard, H. Kröger, and A. Destexhe, Phys. Rev. Lett. **97**, 118102 (2006).
[20] H. Sompolinsky, Phys. Today **41**, 70 (1988).
[21] A. Clauset, C. R. Shalizi, and M. E. J. Newman, SIAM Rev. **51**, 661 (2009).
[22] P. Bak, C. Tang, and K. Wiesenfeld, Phys. Rev. Lett. **59**, 381 (1987).
[23] R. Dickman, A. Vespignani, and S. Zapperi, Phys. Rev. E **57**, 5095 (1998).
[24] R. Dickman, M. A. Muñoz, A. Vespignani, and S. Zapperi, Braz. J. Phys. **30**, 27 (2000).
[25] A. Toib, V. Lyakhov, and S. Marom, J. Neurosci. **18**, 1893 (1998).
[26] S. Marom, Prog. Neurobiol. **90**, 16 (2010).
[27] L. S. Liebovitch, J. Fischbarg, J. P. Koniarek, I. Todorova, and M. Wang, Biochim. Biophys. Acta, Biomembr. **896**, 173 (1987).
[28] G. L. Millhauser, E. E. Salpeter, and R. E. Oswald, Biophys. J. **54**, 1165 (1988).
[29] G. L. Millhauser, E. E. Salpeter, and R. E. Oswald, Proc. Natl. Acad. Sci. USA **85**, 1503 (1988).
[30] For example, the calcium-dependent potassium SK channel [38] is an excitability inhibitor, having a calcium-mediated positive interaction that gives rise to a form similar to that of Eq. (1).
[31] T. E. Harris, Ann. Probab. **2**, 969 (1974).
[32] J. Davidsen and M. Paczuski, Phys. Rev. E **66**, 050101(R) (2002).
[33] B. Englitz, K. M. Stiefel, and T. J. Sejnowski, Neural Comput. **20**, 44 (2008).
[34] B. Naundorf, F. Wolf, and M. Volgushev, Nature (London) **440**, 1060 (2006).
[35] S. Marom and G. Shahaf, Q. Rev. Biophys. **35**, 63 (2002).
[36] P. Dayan and L. F. Abbott, *Theoretical Neuroscience: Computational And Mathematical Modeling of Neural Systems* (MIT Press, Cambridge, MA, 2001), p. 460.
[37] The MATLAB code can be found at http://www.runmycode.org/companion/view/248.
[38] J. P. Adelman, J. Maylie, and P. Sah, Annu. Rev. Physiol. **74**, 245 (2012).